Binding specificity of *Escherichia coli* trigger factor

Holger Patzelt*, Stefan Rüdiger*†, Dirk Brehmer*, Günter Kramer*, Sonja Vorderwülbecke*, Elke Schaffitzel*, Andreas Waitz*, Thomas Hesterkamp*‡, Liying Dong§, Jens Schneider-Mergener§¶, Bernd Bukau*‖, and Elke Deuerling*‖

*Institut für Biochemie und Molekularbiologie, Universität Freiburg, Hermann-Herder-Strasse 7, 79104 Freiburg, Germany; §Institut für Medizinische Immunologie, Universitätsklinikum Charite, Schumannstrasse 20–21, 10098 Berlin, Germany; and ¶Jerini BioTools GmbH, Rudower Chaussee 29, 12489 Berlin, Germany

Edited by Carol A. Gross, University of California, San Francisco, CA, and approved October 12, 2001 (received for review August 15, 2001)

The ribosome-associated chaperone trigger factor (TF) assists the folding of newly synthesized cytosolic proteins in *Escherichia coli*. Here, we determined the substrate specificity of TF by examining its binding to 2842 membrane-coupled 13meric peptides. The binding motif of TF was identified as a stretch of eight amino acids, enriched in basic and aromatic residues and with a positive net charge. Fluorescence spectroscopy verified that TF exhibited a comparable substrate specificity for peptides in solution. The affinity to peptides in solution was low, indicating that TF requires ribosome association to create high local concentrations of nascent polypeptide substrates for productive interaction *in vivo*. Binding to membrane-coupled peptides occurred through the central peptidyl-prolyl-*cis*/*trans* isomerase (PPIase) domain of TF, however, independently of prolyl residues. Crosslinking experiments showed that a TF fragment containing the PPIase domain linked to the ribosome via the N-terminal domain is sufficient for interaction with nascent polypeptide substrates. Homology modeling of the PPIase domain revealed a conserved FKBP(FK506-binding protein)-like binding pocket composed of exposed aromatic residues embedded in a groove with negative surface charge. The features of this groove complement well the determined substrate specificity of TF. Moreover, a mutation (E178V) in this putative substrate binding groove known to enhance PPIase activity also enhanced TF's association with a prolyl-free model peptide in solution and with nascent polypeptides. This result suggests that both prolyl-independent binding of peptide substrates and peptidyl-prolyl isomerization involve the same binding site.

In the *Escherichia coli* cytosol, three chaperones, trigger factor (TF), DnaK, and GroEL, participate in the folding of newly synthesized proteins (1–5). TF associates with the large ribosomal subunit in an apparent 1:1 stoichiometry and crosslinks to short nascent chains of 57 aa (6–8). These findings implicate TF as a prime candidate for the first chaperone to interact with newly synthesized proteins (1).

TF has a modular structure with an N-terminal domain that mediates ribosome binding, a central peptidyl-prolyl-*cis*/*trans* isomerase (PPIase) domain with homology to FK506-binding proteins (FKBPs), and a C-terminal domain with unknown function (6, 9, 10). *In vitro*, both full-length TF and the isolated PPIase domain isomerize peptidyl-prolyl peptide bonds in chromogenic tetrapeptides (6, 10–12). TF also assists the refolding of a model protein, a mutant variant of RNaseT1, which is limited by peptidyl-prolyl isomerization. Refolding is efficiently catalyzed only by full-length TF but not by the isolated PPIase domain (13, 14).

In this study, we investigated (*i*) which sequences in a polypeptide are recognized by TF, (*ii*) whether substrate binding depends on the presence of prolyl residues, and (*iii*) which domains of TF contribute to substrate specificity and substrate binding.

Methods

Synthesis and Screening of Membrane-Bound Peptides. 13meric peptides (overlapping by 10 aa) were synthesized and amino functionalized as previously described (15). Peptides were derived from *E. coli* proteins [EF-Tu (elongation factor Tu), MetE (methionine biosynthesis enzyme), ICDH (isocitrate dehydrogenase), GlnRS (glutamine-tRNA-synthetase), alkaline phosphatase, β-galactosidase, FtsZ (involved in cell division), GBP (galactose-binding protein), L2 (a ribosomal protein), lambda cI, proOmpA (pro-outer membrane protein A), sigma32, and SecA (involved in secretion)] and eukaryotic species [murine DHFR (dihydrofolate reductase), yeast cytochrome B2, F1β- and Su9-ATPase subunits, *Photinus pyralis* luciferase, RNaseT1 from *Aspergillus oryzae*, and human PrP (prion protein)]. Screening was performed according to ref. 16. Peptide libraries were incubated with 500 nM TF or 5 μM TF fragments. Bound chaperone was electrotransferred to a poly(vinylidene difluoride) membrane and immunodetected.

Development of the Prediction Algorithm. Sequences from adjacent overlapping peptides with high affinity for TF were created and aligned (16). For each amino acid and its position in the consecutive peptide stretches the Gibbs free enthalpy was calculated according to the equation: $\Delta\Delta G_K = -RT\ln(P_b/P_n)$, P_b and P_n being the relative occurrence of each amino acid in the bound peptide stretch and in nonbinding peptides, respectively. According to ref. 16, to each 13meric peptide a score value was assigned as a measure of the likelihood to bind TF. A cutoff for binding peptides was set at −5 because 85% of high affinity binders had a score value below −5. Next, energy values were varied for the amino acids that were either enriched (Phe, Tyr, Trp, His, Arg, and Lys) or disfavored (Glu and Asp) in high affinity binders to improve prediction until the predicted binding property was best in comparison with experimental data. In addition the number of amino acids included in the calculation was varied. An average value over all motif positions for every amino acid revealed the optimal result (averaged values as follows: A, 0.5; C, −0.2; D, 1.0; E, 1.2; F, −3.2; G, 0.3; H, −2.2; I, −0.9; K, −0.6; L, −0.5; M, 0.8; N, −0.3; P, −0.1; Q, 0.0; R, −1.2; S, 0.2; T, 0.7; V, −0.1; W, −1.8; and Y, −3.6).

Mutant Construction and Protein Purification. TF-E178V was created by using the plasmid pDS56-*tig*-his$_6$ (9) and the QuikChange Site-Directed Mutagenesis Kit from Stratagene. TF, TF fragments, and TF-E178V were purified and checked for structural integrity (9).

Peptide Binding Studies in Solution. The complex formation of TF or TF-E178V and peptide substrate was measured by using a fluorescent-labeled peptide (F-pep1). This peptide (pep1, *E. coli* σ^{32}-Q132-Q144-C) was labeled with IAANS [2-(4-iodoacetamido)anilino-naphtalene-6-sulfonic acid] as described (17). TF

This paper was submitted directly (Track II) to the PNAS office.

Abbreviations: TF, Trigger Factor; PPIase, peptidyl-prolyl-*cis*/*trans* isomerase; FKBP, FK506 binding protein; ICDH, isocitrate dehydrogenase.

†Present address: Cambridge Centre for Protein Engineering, Medical Research Council Centre, Hills Road, Cambridge, United Kingdom CB2 2QH.

‡Present address: EVOTEC BioSystems AG, D-22525 Hamburg, Germany.

‖To whom reprint requests should be addressed. E-mail: deuerli@uni-freiburg.de and bukau@uni-freiburg.de.

The publication costs of this article were defrayed in part by page charge payment. This article must therefore be hereby marked "*advertisement*" in accordance with 18 U.S.C. §1734 solely to indicate this fact.

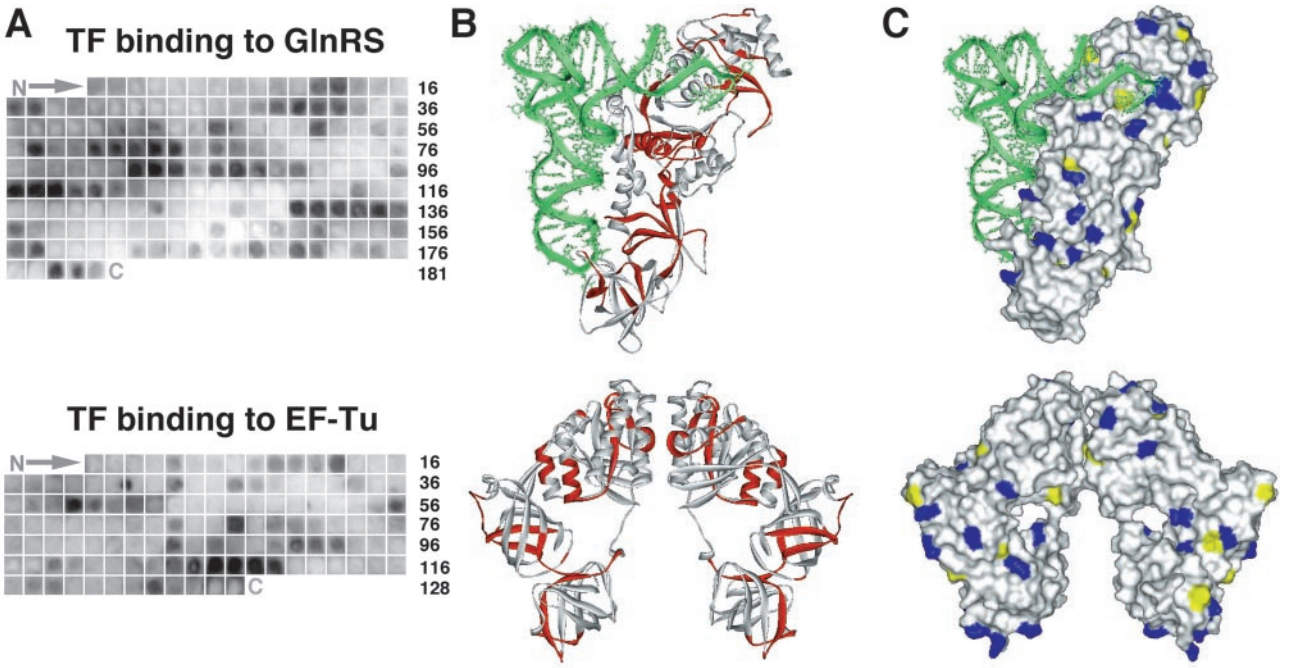

Fig. 1. TF binding to peptide libraries and localization of binding sites in native protein structures. (*A*) Binding of TF to 13meric peptide libraries derived from EF-Tu (elongation factor-Tu) and GlnRS (glutamine-tRNA-synthetase). Numbers at the right indicate the last peptide spot in the row. (*B*) Ribbon and (*C*) space filling representations (WEBLABVIEWER) of the structures of the corresponding native proteins [GlnRS in complex with its tRNA (green), dimer of EF-Tu]. Red segments in *B* correspond to the peptides bound with high affinity on the library in *A*. (*C*) Aromatic and positively charged residues within the binding sites are shown in yellow and blue, respectively.

or TF-E178V (1.5 μM) was incubated with 1.5 μM F-pep1 in F-buffer (20 mM Tris·HCl, pH 7.5/100 mM NaCl/0.5 mM EDTA) for 1 h at 30°C. For competition experiments, 100 μM unlabeled pep1, pep2 (σ^{32}-K4-L16, KMQSLALAPVGNL), or pep3 (σ^{32}-derived, QGNIGLMKAVRRF) were mixed with the preformed TF-F-pep1 complex (each 1.5 μM) and incubated in F-buffer for 1 h at 30°C. The fluorescence emission spectra were measured from 350 to 600 nm after excitation at 335 nm. For determination of the K_D values for TF and the TF-E178V mutant, 0.7 μM and 0.3 μM F-pep1, respectively, were incubated with increasing concentrations of TF (1–120 μM) and TF-E178V (1–200 μM) for 1 h at 30°C in F-buffer. The observed fluorescence intensities at the emission maximum of 450 nm (after excitation at 335 nm) were plotted against the protein concentrations and fitted by a quadratic equation by using the GRAFIT program, version 5.0.1. All experiments were repeated at least three times.

***In Vitro* Transcription/Translation and Chemical Crosslinking.** Extracts from *E. coli* Δ*tig* cells and arrested nascent chains were generated as described (18). For production of nascent ICDH, the gene was cloned from *E. coli* by PCR technique (primers I5′ acgtccatggaaagtaaagtagttgttccg and I3′ cgggatccttacatgttttcgatgatcgcg). The product was inserted via *Nco*I and *Bam*HI sites into pET3d. Transcription was started with 2 ng/μl pET-ICDH. Arrested nascent chains were produced by addition of 40 ng/μl antisense-oligonucleotide (5′-cccccatctcttcacgcagg-3′). Translation extracts were supplemented with 7.5 units of T7 RNA-polymerase and 0.3 μCi/μl [^{35}S]methionine. After 30 min, crosslinker disuccinimidyl suberate (2.5 mM) was added for 30 min at room temperature, the reaction was quenched with 50 mM Tris·HCl (pH 7.5) for 15 min at room temperature, and ribosomal complexes were purified (9) and coimmunoprecipitated (19). For release of nascent polypeptides, 1 mM puromycin was added after translation and incubated 15 min on ice. By centrifugation (20 min, 150,000 × *g*, 4°C), the ribosomes were separated, and the supernatant was used for chemical crosslinking and coimmunoprecipitation.

Results

Substrate Specificity of Trigger Factor. We determined the binding motif of TF by screening 2,842 membrane-coupled peptides scanning the sequences of 20 proteins originating from different species for binding to TF. The scans were composed of 13meric peptides, which overlapped by 10 residues and therefore represented all potential linear binding sites in the proteins. They were incubated to equilibrium with purified TF followed by electrotransfer and immunodetection of the chaperone. Membrane-coupled peptides are particularly suitable for such analysis because (*i*) TF accepts peptides as surrogate ligands (6, 10), (*ii*) peptides irrespective of their hydrophobicity and hence solubility can be investigated, and (*iii*) the peptides mimic short nascent polypeptide chains emerging from the ribosomal tunnel that are known to interact with TF (6, 8). Fig. 1*A* shows two examples of the peptide scans. TF bound only to a subset of peptides and thus differentiated between amino acid side chains. Binding sites occurred frequently (about every 32 residues) in all protein sequences tested. The frequency of binding was independent of origin, size, and oligomeric state of the proteins analyzed. Binding sites were not clustered at the N terminus or elsewhere in the protein sequences. The localization of TF binding sites in several proteins of known three-dimensional structure was determined. Fig. 1*B* shows glutamine tRNA-synthetase and EF-Tu as examples. In most cases, TF binding sites were buried within the hydrophobic interior of the molecules, and only some binding sites exposed single residues (usually charged residues) at the protein surface (Fig. 1*C*). Furthermore, by investigating the occurrence of binding sites in secondary structure elements, we found that TF has a preference neither for α-helices nor for β-strands or other structural elements (data not shown).

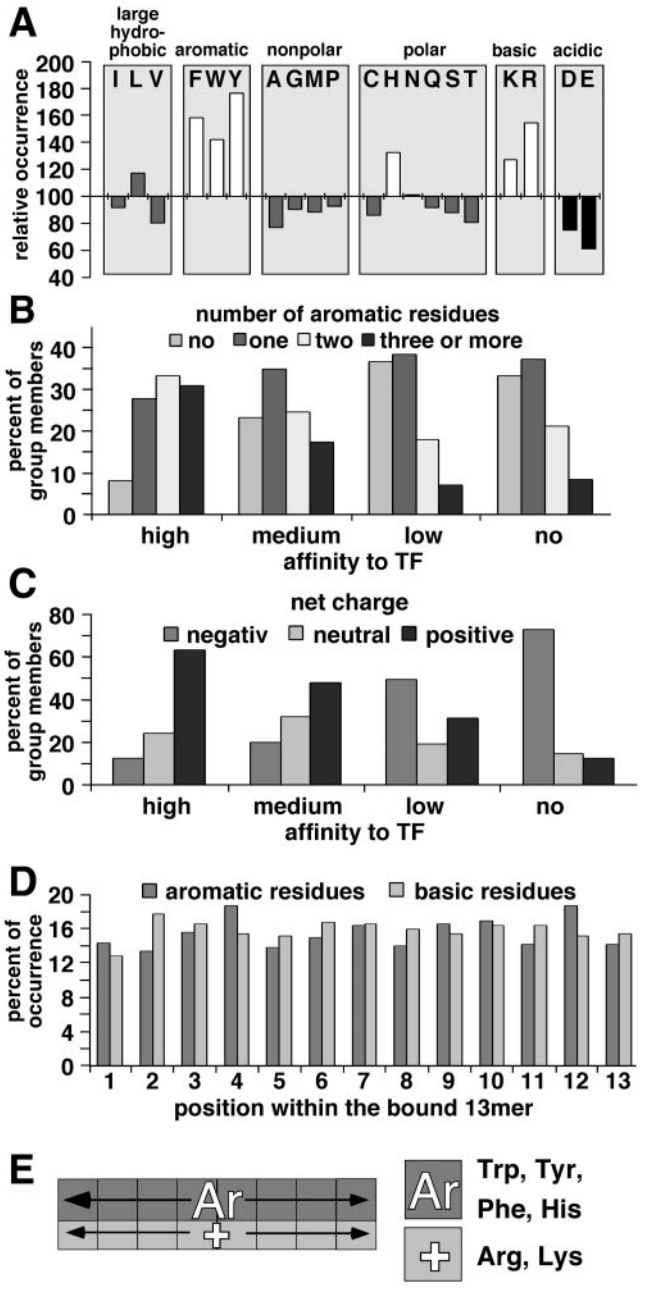

Fig. 2. Substrate specificity of TF. (*A*) For 2,842 peptides representing 20 protein sequences, the relative amino acid occurrence was determined. The relative occurrence of each amino acid in TF binding peptides with high affinity is normalized to its occurrence in the whole peptide libraries (set as 100%). Classifications of high, medium, low, and no affinity binders according to the occurrence of aromatic side chains (*B*) and the net charge (*C*). Positioning of enriched aromatic and basic residues within the 13meric peptides with high affinity for TF (*D*). TF recognition motif (*E*).

The large data set we obtained allowed a reliable statistical analysis. All screened peptides were grouped into four classes according to their affinity for TF as determined by fluoroimager quantification of signals: high (508 peptides), medium (689), and low (816) affinity binders and non-binders (829). Comparison of the relative occurrences of the 20 aa in the total libraries and the peptides bound with high affinity showed that these peptides were highly enriched in aromatic (Phe, Tyr, Trp, and His) and positively charged (Arg and Lys) residues, whereas negatively charged (Asp and Glu) residues were disfavored (Fig. 2*A*). Among the 508 peptides with high affinity for TF, only 8% lacked aromatic residues, whereas 64% contained two or more aromatic residues (Fig. 2*B*). With regard to the net charge of bound peptides, it is interesting that 63% of the high affinity binders had a positive net charge $\geq +1$ (Fig. 2*C*). In contrast, among the 829 non-binders, 33% lacked aromatic residues, only 30% contained more than one, and 73% had a negative net charge ≤ -1. Furthermore, no specific positioning of enriched aromatic and basic residues was found within the 13meric peptides with high affinity for TF (Fig. 2*D*) and no preferred spacing between aromatic and basic residues was present in these peptides (not shown). Statistical analysis of the peptides with medium affinity for TF showed qualitatively similar results as the high affinity binders.

TF is an acidic protein and therefore binding to positively charged residues may be envisioned as unspecific association. One would expect two populations of bound peptides with a minor overlap: positively charged peptides and peptides enriched in aromatic residues. However, in 92% of the bound peptides, the positive net charge is linked to the presence of one or more aromatic residues. The possibility that the preference for aromatic residues simply reflects a nonspecific hydrophobic interaction can also be ruled out because Ile and Val are not enriched in binding peptides.

Interestingly, prolines did not contribute to substrate binding (Fig. 2*A*). Fifty-five percent of the binding peptides did not even contain prolines, demonstrating that this amino acid is not required for association of TF with peptides. This result is in agreement with the earlier finding from Schmid and coworkers, who showed that TF binding to the model substrate RNaseT1 is independent of prolyl residues (20). On the basis of our statistical analysis, we suggest that TF in general binds peptides independent of the presence of prolyl residues.

Binding Motif for Trigger Factor and Prediction Algorithm. The size of the dataset collected allowed the determination of a TF binding motif and the subsequent development of an algorithm to predict TF binding sites in peptide sequences. The best prediction, with >80% accuracy, was obtained for a motif of eight consecutive amino acids, among which aromatic and basic residues were favored and acidic residues were disfavored, whereby the positions of these residues within the motif were not important (Fig. 2*E*). For our TF algorithm, the net charge of the peptide was parametrized because TF preferred binding to peptides with a positive net charge. It is important to note that, although the 8mer motif is suitable for predicting TF binding sites, TF may bind peptide sequences either longer or shorter than eight amino acids.

The PPIase Domain of Trigger Factor Mediates Peptide Binding. Given the curious result that TF binding to peptides was independent of prolyl residues, we tested whether the PPIase domain was involved in this peptide binding. We performed peptide scans by using recombinant fragments of TF containing the N-terminal domain TF (1–144), the central PPIase domain TF (145–247), the C-terminal domain TF (248–432), and combinations of these fragments (Fig. 3*A*). TF (248–432) was too unstable to be analyzed on its own. We found that the PPIase domain alone (Fig. 3*B*) or the fragments TF (1–247) and TF (145–432), which contained the PPIase domain, showed significant affinity to the peptides on the cellulose membrane and exhibited a specificity similar to full-length TF. In contrast, the N-terminal domain did not show specific peptide binding (not shown). It is important to stress that, for all fragments, a ten-fold higher protein concentration was used as compared with full-length TF. This result was at least partially due to the reduced recognition of the fragments by the polyclonal antisera raised against full-length TF. In addition, it suggests that the affinity of the isolated PPIase

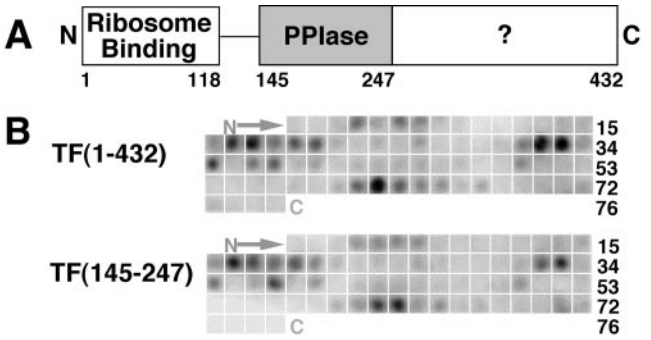

Fig. 3. Peptide binding is mediated by TF's PPIase domain. (*A*) Domain organization of TF. (*B*) Comparative peptide scans (*E. coli* Lambda cI protein) after incubation with full-length TF (1–432) and the PPIase domain TF (145–247).

domain toward peptides is lower. The specificity, however, mediated by the PPIase domain was independent of prolyl residues because the peptide binding spots 17 to 20 and 62 to 63 (Fig. 3*B*) did not contain prolines. We conclude that peptide binding by TF occurs through the PPIase domain and does not require the presence of prolyl residues in the bound peptide.

Interaction of TF with Peptides in Solution. To analyze whether TF displays the same substrate specificity for peptides in solution, we chose a prolyl-free model peptide (pep1, QRKLFFNLRKTKQC), which was identified as a high affinity binder in the peptide scans. This peptide was labeled with IAANS (F-pep1), and peptide binding was monitored by the change in fluorescence. Complex formation between TF and F-pep1 was detected by a strong increase in fluorescence as shown in Fig. 4*A*. The fluorescence of a preformed complex of TF with the substrate (F-pep1) could be quenched with a 60-fold excess of unlabeled pep1, but not with pep2 or pep3, which were non-binders on the libraries [pep2, KMQSLALAPVGNL (see Fig. 4*A*); pep3, QGNIGLMKAVRRF, data no shown]. Thus the substrate specificity of TF determined by scanning cellulose-bound peptides is similar to TF's specificity for peptides in solution.

Trigger Factor's Affinity for Peptides Is Low. For determination of the K_D, we titrated F-pep1 with TF. The resulting fluorescence intensities (450 nm) were plotted against increasing TF concentrations and fitted by a quadratic equation (Fig. 4*B*). The calculated K_D was $\approx$120 μM. Obviously, TF's affinity for pep1 is low, and the interaction in solution is weak. Comparably high K_D values for peptides were also observed for other PPIases. The *E. coli* FKBP-like FkpA isomerase binds to a tetrapeptide substrate with an estimated K_D of 730 μM (21), and the K_D for association of the cyclophilin Cyp18 with a tetrapeptide is 220 μM as determined by NMR spectroscopy (22). It is important to notice here that the very high peptide density of peptides spotted on libraries (200 nmol/mm^2) creates an actual peptide concentration within a spot by far high enough to allow the binding of detectable amounts of TF.

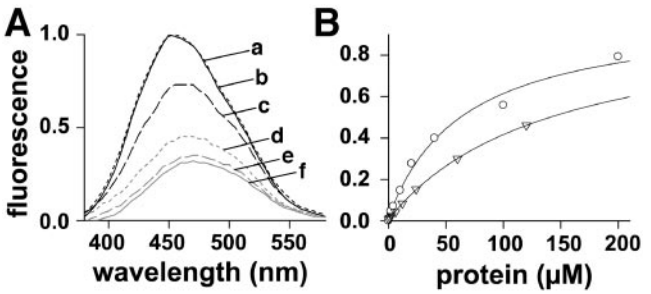

Fig. 4. Interaction of TF with peptides in solution. (*A*) Fluorescence measurements of TF and F-pep1 (a, black solid line), of TF and F-pep1 quenched with a 60-fold excess of unlabeled pep1 (c, black dashed line), and of TF and F-pep1 with a 60-fold excess of the nonbinding pep2 (b, black dotted line). Fluorescence signals of F-pep1 alone (f, gray solid line) and of F-pep1 together with pep1 (e, gray dashed line) or pep2 (d, gray dotted line) are shown for control. The highest fluorescence amplitude was set as 1. (*B*) Titration of TF (triangles) and TF-E178V (circles) against F-pep1 for K_D determination of both protein-F-pep1 complexes (the calculated maximum fluorescence was set as 1 for both).

Prolyl-Independent Peptide Binding and Peptidyl-Prolyl Isomerization Colocalize. To demonstrate that peptide binding in solution also occurs via the PPIase domain of TF, we could not make use of FK506 or other PPIase inhibitors to block the binding pocket because *E. coli* TF does not bind them. Furthermore, no specific fluorescence signal of F-pep1 in complex with each of the single domains of TF or domain combinations [TF (1–247) or TF (145–432)] was obtained.

As an alternative approach, we searched for mutations in the PPIase domain that would influence peptide binding without disturbing the structure. Introducing mutations that lead to even lower affinities for peptides would cause difficulties to determine K_D values because the appropriate range of high concentrations could not be achieved. Therefore, we looked for a TF mutant with enhanced peptide affinity. We took advantage of a previous study by Fischer and coworkers (23). They introduced several single point mutations in conserved amino acid residues that were proposed to form an FKBP-like binding pocket where peptidyl-prolyl isomerization takes place. The mutation E178 to V was reported to cause a 1.6-fold increase in PPIase activity toward a tetrapeptide. This could be due to either enhanced catalytic activity or increased peptide binding. We created the mutant TF-E178V and confirmed, by CD spectra, partial proteinase K digest and gel filtration, that the overall structural integrity was as published for TF (9, 14). Like the wild-type protein, the TF-E178V mutant displayed a fluorescence signal with F-pep1, which could be quenched with unlabeled pep1, but not with pep2 or pep3 (data not shown). We determined a K_D of $\approx$60 μM (Fig. 4*B*). The E178V mutation thus enhanced the affinity to the prolyl-free pep1 2-fold. This finding supports our conclusion that the proposed substrate binding pocket in the PPIase domain is responsible for the interaction of TF with peptides, and that this interaction does not require the presence of prolines in the substrate.

Interaction with Nascent Polypeptides. To verify the involvement of the PPIase domain for binding to nascent polypeptide substrates, we generated arrested ^{35}S-labeled nascent chains of ICDH in an *in vitro* transcription/translation system derived from a TF knockout *E. coli* strain. This polypeptide was 173 aa long and contained two potential binding sites for TF as determined by scanning of the peptide library (data not shown). Extracts were supplemented with either TF (1–432) wild type or TF-E178V in a physiological ratio to ribosomes (3:1). After translation, nascent chains were crosslinked to TF variants by using the chemical crosslinker disuccinimidyl suberate. TF crosslinking products were identified by coimmunoprecipitation with TF-specific antibodies. As shown in Fig. 5, the mutant TF-E178V, displaying enhanced affinity for soluble peptides, also revealed increased crosslinking efficiency compared with wild-type TF (Fig. 5, lanes 8 and 11). We conclude that binding to nascent substrates involves the PPIase domain.

The low affinity of TF for peptides in solution suggests that TF may require ribosome association to create a high local concentration of the nascent polypeptide substrate. We supplemented

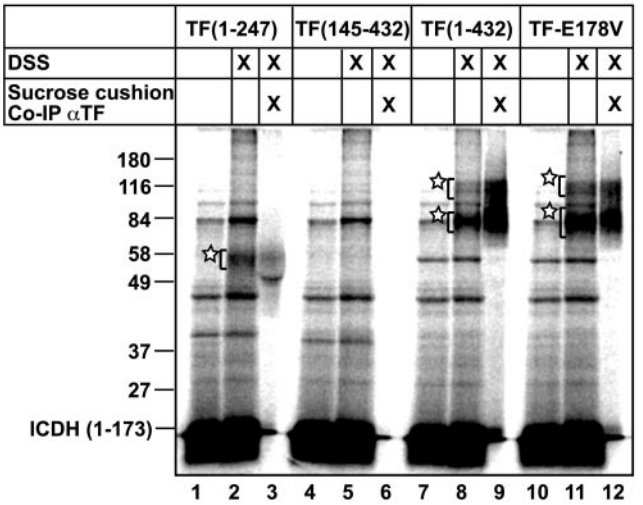

Fig. 5. Interaction of TF with nascent polypeptides. Arrested ^{35}S-labeled nascent ICDH was synthesized *in vitro* in a TF-deficient transcription/translation system supplemented with TF fragments, TF (1–432) wild type, or TF-E178V. Minor bands visible in the autoradiography correspond to either residual full-length ICDH or endogenous background products of unknown identity. After crosslinking with disuccinimidyl suberate (lanes 2, 5, 8, and 11) and sucrose cushion centrifugation, ribosome-nascent chain complexes were coimmunoprecipitated to identify TF crosslinks (lanes 3, 6, 9, and 12). Brackets with stars indicate crosslinking products of TF variants. In lane 3, the bulky band of IgGs in the antisera comigrates with the radiolabeled crosslinking product and shifts part of it to lower molecular weight. Please note that TF (1–247) and TF-E178V are less efficiently recognized by TF antibodies as compared with wild-type TF.

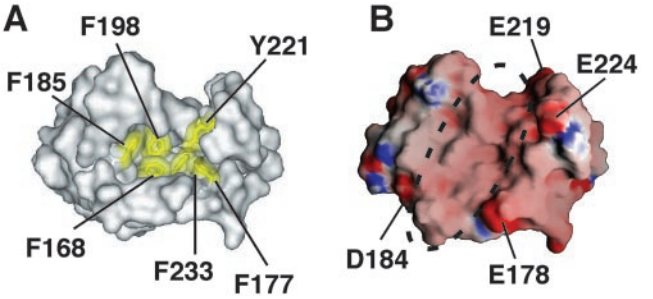

Fig. 6. Homology modeling of TF's PPIase domain TF (145–242) based on the yeast FKBP12 structure by using INSIGHT II. (*A*) Model illustrated by WEBLAB-VIEWER. The stick representation shows the conserved aromatic residues of the FKBP-like binding pocket (yellow), numbered by their position in full-length TF. (*B*) Surface charge illustration of the model by using GRASP. Red color represents negative surface charges and blue color positive surface charges (increasing intensity indicates increasing charge). Negatively charged residues at the border of the groove are labeled with their positions in the full-length protein. The dashed circle indicates the putative binding groove of this domain embedding the conserved aromatic residues of the binding pocket as shown in *A*.

the transcription/translation system with the TF fragment TF (1–247) or TF (145–432). Both fragments contain the PPIase domain but lack either the C-terminal domain or the N-terminal ribosome binding domain. The non-ribosome-associated fragment TF (145–432) could not be crosslinked to the nascent chain (Fig. 5, lanes 5 and 6). In contrast, the ribosome-bound fragment TF (1–247) was sufficient for crosslinking to the nascent polypeptide (Fig. 5, lanes 2 and 3). Crosslinking efficiency was lower as for full-length TF (lanes 8 and 9), and only one crosslink adduct could be observed. Moreover, release of nascent chains by puromycin before crosslinking abolished the association of full-length TF with polypeptide substrates (data not shown).

Taken together, we conclude that (*i*) the TF PPIase domain contributes to the interaction with nascent polypeptides and (*ii*) ribosome association is a prerequisite for TF binding to nascent chains.

Discussion

In this study, we show that (*i*) TF recognizes aromatic and basic amino acid residues in peptide substrates, (*ii*) TF binding to peptides does not depend on the presence of prolines, and (*iii*) prolyl-independent substrate binding and catalytic PPIase activity involve the same binding site within the PPIase domain of TF.

The substrate specificity of TF was determined by scanning cellulose-bound peptides. We verified that TF interacts with a peptide in solution, which was identified as a binder in the peptide scans, and that TF does not interact with two peptides that were non-binders. TF recognized an 8-aa stretch enriched in aromatic and basic residues without position specificity. This situation is comparable to the DnaK chaperone binding motif, which consists of a hydrophobic core of 5 aa flanked by positively charged residues. Within this hydrophobic core no specific positioning of residues is required. Compared with the TF motif, however, the hydrophobic core of the DnaK motif is shorter, and aliphatic residues are preferred (16). In contrast to DnaK, TF does not show a preference for positively charged amino acids at the flanking regions of the core.

Interestingly, peptide binding on the libraries was independent of prolyl residues. In solution, we showed that a prolyl-free model peptide associates with TF. The general contribution of prolyl residues to peptide binding is difficult to investigate in solution. A reliable statistical analysis is impossible because large K_D data sets cannot be obtained. In contrast, the investigation of TF binding to 2,842 membrane-bound peptides allowed us to provide a large data set that established the generality of TF's prolyl-independent substrate recognition.

From a mechanistic point of view, prolyl-independent substrate recognition and PPIase activity could be linked; TF might bind to regions enriched in aromatic residues and then scan for adjacent prolyl residues to be isomerized in the substrate. However, this mechanism would render TF as a very inefficient enzyme because 55% of bound peptides do not contain a prolyl residue.

As shown here, the association of TF with peptides in solution is weak. Because of the high K_D of TF-pep1 complex formation, we consider it very unlikely that TF interacts with peptides in solution in the cell. How can ribosome-associated TF then interact efficiently with short nascent polypeptides? We speculate that the localization of TF on the ribosome next to the exit site of emerging polypeptides is crucial to create a local concentration high enough for TF to bind nascent chains. This idea is supported by the crosslinking experiment in our *in vitro* translation system supplemented with a physiological 3-fold excess of TF variants over ribosomes. A TF fragment lacking the ribosome-binding domain did not crosslink to nascent ICDH. Furthermore, for released nascent polypeptides, no crosslinking product with wild-type TF could be observed. The low affinity for peptides in solution may reflect the local sphere of action of TF and at the same time may prevent the chaperone from being titrated out by peptides or misfolded proteins generated in the cytosol.

We showed that substrate binding is mediated by the PPIase domain of TF by using three independent approaches. First, the PPIase domain is sufficient for binding to peptide libraries with the same specificity as full-length TF. Second, the TF-E178V PPIase mutant revealed an increased affinity toward a prolyl-free model peptide as well as enhanced crosslinking efficiency to nascent substrates as compared with wild-type TF. Third, the

fragment TF (1–247) that contains the PPIase domain and the N-terminal domain crosslinks to ICDH nascent polypeptides and all other nascent polypeptides tested so far (PykF, pyruvate kinase; OmpA, outer membrane protein A; S.V. and B.B., unpublished results). For the N-terminal domain TF (1–144) alone, however, crosslinking results were inconsistent. This fragment could be crosslinked to nascent ICDH (data not shown), whereas for nascent OmpA no crosslinking product could be observed, and nascent PykF crosslinking revealed a broad smear. Further experiments are required to elucidate the contribution of the N-terminal domain to the interaction with nascent chains.

Binding of our model peptide pep1 to the isolated PPIase domain could not be monitored in solution. Different explanations are possible: the N- and C-terminal domains could be necessary for interaction with the fluorescent dye although they do not contribute to substrate specificity. A similar finding is described for a DnaK mutant protein, which lacks the helical lid enclosing the substrate binding pocket (24). Alternatively, the flanking domains of the PPIase domain may contribute to the affinity for the substrate. This hypothesis is supported by our experiments showing that (*i*) a 10-fold higher concentration of the isolated PPIase domain is necessary to observe binding to peptide libraries and (*ii*) the crosslinking efficiency of the TF (1–247) fragment is lower as compared with full-length TF. Furthermore, it is consistent with the finding that efficient binding and refolding of RNaseT1 required all three domains of TF (14). The lower affinity for substrates can be explained by assuming that the N- and C-terminal domains (*i*) provide unspecific (e.g., backbone) contacts to the substrate or (*ii*) modulate the accessibility or conformation of the PPIase binding pocket. The latter case was reported in a recent publication showing that domains adjacent to the PPIase domain in large FKBPs can alter the stability of these proteins (25).

Can the substrate specificity of the PPIase domain be understood by its structural properties? Because no structural information about TF is available so far, we modeled TF's PPIase domain based on the structure of the homologous PPIase FKBP12 from *Saccharomyces cerevisiae* (28.6% protein sequence identity, 53.1% similarity; ref. 26). The model shows that the key residues forming the FKBP12 substrate-binding pocket are also conserved in the TF domain. The modeled pocket consists of six aromatic amino acids providing a hydrophobic surface for substrate interaction (Fig. 6*A*). Surface charge representation (Fig. 6*B*) reveals that the hydrophobic pocket is embedded in a negatively charged putative groove with a right border (in standard view) built by three residues (E178, E219, and E224) and a negatively charged residue at the left border (D184). It is conceivable that this groove is able to bind peptides enriched in aromatic and basic amino acids as found in the TF binding motif. The preference of TF for positively charged peptides is complementary with the negative charge of this groove. The enrichment of aromatic amino acids in the bound peptides is explained by a hydrophobic interaction of their side chains with the exposed aromatic residues in the central pocket of the groove. The enhanced affinity of TF-E178V toward our model peptide might be due to the increased hydrophobicity at the border of the binding pocket whereas the residues D184, E219, and E224 maintain the overall negative charge of the groove. We propose that this groove unifies both the prolyl-independent binding of peptide substrates and the catalytic isomerase activity.

The importance of the PPIase activity of TF for the folding of newly synthesized proteins remains unclear. The TF substrate specificity suggests that the PPIase domain has a more general, chaperone-like activity *in vivo*. Chaperone-like activities independent of PPIase activities have been reported for other PPIases of the FKBP family (25, 27). Why does TF specifically recognize aromatic residues and not hydrophobic residues in general as DnaK does? We speculate that the binding of TF may protect nascent polypeptides enriched in aromatic and basic amino acids against unproductive association with ribosomal RNA. The negative charge of the RNA and the aromatic ring systems of its bases may interact with these stretches in nascent chains in the absence of TF and thereby disturb the translation or folding process.

We thank D. Dougan, M. P. Mayer, and K. Turgay for comments on the manuscript. This work was supported by grants from the Deutsche Forschungsgemeinschaft (SFB 388, Graduiertenkolleg) to B.B. and E.D. and the Fonds der Chemischen Industrie to B.B.

1. Bukau, B., Deuerling, E., Pfund, C. & Craig, E. A. (2000) *Cell* **101,** 119–122.
2. Ellis, R. J. & Hemmingsen, S. M. (1989) *Trends Biochem. Sci.* **14,** 339–342.
3. Gething, M.-J. H. & Sambrook, J. F. (1992) *Nature (London)* **355,** 33–45.
4. Hartl, F. U. (1996) *Nature (London)* **381,** 571–580.
5. Horwich, A. L., Brooks Low, K., Fenton, W. A., Hirshfield, I. N. & Furtak, K. (1993) *Cell* **74,** 909–917.
6. Hesterkamp, T., Hauser, S., Lütcke, H. & Bukau, B. (1996) *Proc. Natl. Acad. Sci. USA* **93,** 4437–4441.
7. Lill, R., Crooke, E., Guthrie, B. & Wickner, W. (1988) *Cell* **54,** 1013–1018.
8. Valent, Q. A., de Gier, J.-W. L., von Heijne, G., Kendall, D. A., ten Hagen-Jongman, C. M., Oudega, B. & Luirink, J. (1997) *Mol. Microbiol.* **25,** 53–64.
9. Hesterkamp, T., Deuerling, E. & Bukau, B. (1997) *J. Biol. Chem.* **272,** 21865–21871.
10. Stoller, G., Ruecknagel, K. P., Nierhaus, K. H., Schmid, F. X., Fischer, G. & Rahfeld, J.-U. (1995) *EMBO J.* **14,** 4939–4948.
11. Stoller, G., Tradler, T., Rucknagel, K. P., Rahfeld, J.-U. & Fischer, G. (1996) *FEBS Lett.* **384,** 117–122.
12. Hesterkamp, T. & Bukau, B. (1996) *FEBS Lett.* **385,** 67–71.
13. Scholz, C., Stoller, G., Zarnt, T., Fischer, G. & Schmid, F. X. (1997) *EMBO J.* **16,** 54–58.
14. Zarnt, T., Tradler, T., Stoller, G., Scholz, C., Schmid, F. X. & Fischer, G. (1997) *J. Mol. Biol.* **271,** 827–837.
15. Volkmer-Engert, R., Hoffmann, B. & Schneider-Mergener, J. (1997) *Tetrahedron Lett.* **38,** 1029–1032.
16. Rüdiger, S., Germeroth, L., Schneider-Mergener, J. & Bukau, B. (1997) *EMBO J.* **16,** 1501–1507.
17. McCarty, J. S., Rüdiger, S., Schönfeld, H.-J., Schneider-Mergener, J., Nakahigashi, K., Yura, T. & Bukau, B. (1996) *J. Mol. Biol.* **256,** 829–837.
18. Schaffitzel, E., Rüdiger, S., Bukau, B. & Deuerling, E. (2001) *Biol. Chem.* **382,** 1235–1243.
19. Deuerling, E., Schulze-Specking, A., Tomoyasu, T., Mogk, A. & Bukau, B. (1999) *Nature (London)* **400,** 693–696.
20. Scholz, C., Mücke, M., Rape, M., Pecht, A., Pahl, A., Bang, H. & Schmid, F. X. (1998) *J. Mol. Biol.* **277,** 723–732.
21. Arié, J.-P., Sassoon, N. & Betton, J.-M. (2001) *Mol. Microbiol.* **39,**199–210.
22. Kofron, J. L., Kuzmic, P., Kishore, V., Colon-Bonilla, E. & Rich, D. H. (1991) *Biochemistry* **30,** 6127–6134.
23. Tradler, T., Stoller, G., Rücknagel, K. P., Schierhorn, A., Rahfeld, J.-U. & Fischer, G. (1997) *FEBS Lett.* **407,** 184–190.
24. Mayer, M. P., Schröder, H., Rüdiger, S., Paal, K., Laufen, T. & Bukau, B. (2000) *Nat. Struct. Biol.* **7,** 586–593.
25. Pirkl, F. & Buchner, J. (2001) *J. Mol. Biol.* **308,** 795–806.
26. Rotonda, J., Burbaum, J. J., Chan, H. K., Marcy, A. I. & Becker, J. W. (1993) *J. Biol. Chem.* **268,** 7607–7609.
27. Ramm, K. & Plückthun, A. (2000) *J. Biol. Chem.* **275,** 17106–17113.